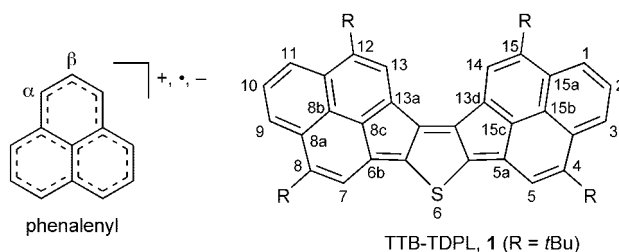


Four-Stage Amphoteric Redox Properties and Biradicaloid Character of Tetra-*tert*-butyldicyclopenta[*b*; *d*]thieno[1,2,3-*cd*;5,6,7-*c'**d'*]diphenylene**

Takashi Kubo,* Maki Sakamoto, Minako Akabane, Yoshinori Fujiwara, Kageyoshi Yamamoto, Motoko Akita, Katsuya Inoue, Takeji Takui, and Kazuhiro Nakasuji*

Dedicated to Emeritus Professor Ichiro Murata on the occasion of his 75th birthday

Phenalenyl-based hydrocarbons possess highly amphoteric redox properties that give low oxidation and high reduction potentials and afford stable multivalent redox species.^[1] These



α -position: 1,3,4,5a,6b,8,9,11,12,13a,13d,15
 β -position: 2,5,7,10,13,14

compounds have frontier orbitals with a nonbonding molecular orbital (NBMO) character that results from a weak perturbation between singly occupied molecular orbitals (SOMOs) of the phenalenyl radical and the frontier orbitals of a central conjugated system. This perturbation leads to a

[*] Dr. T. Kubo, M. Sakamoto, M. Akabane, Y. Fujiwara, Prof. Dr. K. Yamamoto, Prof. Dr. K. Nakasuji
 Department of Chemistry
 Graduate School of Science, Osaka University
 Machikaneyama 1-1, Toyonaka, Osaka 560-0043 (Japan)
 Fax: (+81) 6-6850-5395
 E-mail: kubo@chem.sci.osaka-u.ac.jp
 nakasuji@chem.sci.osaka-u.ac.jp

Dr. M. Akita, Prof. Dr. K. Inoue
 Department of Applied Molecular Science
 Institute for Molecular Science
 Okazaki 444-8585 (Japan)

Prof. Dr. T. Takui
 Departments of Chemistry and Materials Science
 Graduate School of Science, Osaka City University
 Sumiyoshi-ku, Osaka 558-8585 (Japan)

[**] This work was supported by a Grant-in-Aid for Scientific Research on Priority Areas (No. 15750034, Area No. 769, Proposal No. 15087202) from the Ministry of Education, Culture, Sports, Science, and Technology (MEXT), Japan.



Supporting information for this article is available on the WWW under <http://www.angewandte.org> or from the author.

small gap between the highest occupied molecular orbital (HOMO) and the lowest unoccupied molecular orbital (LUMO). This amphoteric redox property makes the phenalenyl moiety an important species in redox chemistry. Herein, the synthesis and properties of a new phenalenyl-based conjugated system that has amphoteric redox properties (Scheme 1) and a biradicaloid character originating from a small HOMO–LUMO gap is reported.

The synthetic procedure for **1** is shown in Scheme 2. The key intermediates **3** were obtained as an isomeric mixture of 3,10-, 3,11-, and 4,10-dimethyl compounds by treatment of acenaphthene derivative **2** with sulfur.^[2] Isolation of the individual isomers was not carried out as **1** could be prepared from each of them. Bis(propionic acid) derivatives **6** were obtained in three steps. Intramolecular Friedel–Crafts cyclization of the acyl chloride of **6** with AlCl₃ gave diketones **7**, which were reduced and subsequently dehydrated to afford dihydro compounds **9**. Dehydrogenation of **9** with *p*-benzoquinone provided the target compound **1** as black prisms. Compound **1** was found to be stable in the solid state at room temperature even in air. The structure of **1** was confirmed by X-ray crystographic analysis (see below).

The cyclic voltammogram of **1** gave four reversible redox waves, with two oxidation potentials ($E_2^{\text{ox}} = +0.94$ V and $E_1^{\text{ox}} = +0.47$ V) and two reduction potentials ($E_1^{\text{red}} = -0.53$ V and $E_2^{\text{red}} = -0.90$ V; Figure 1). The reversibility of the redox waves indicates the persistency of the mono- and divalent ionic species. Furthermore, the low E_1^{ox} and high E_1^{red} values suggest that the oxidized and reduced species that are generated have high thermodynamic stabilities. The E_1^{sum} value^[3a] of 1.00 V is

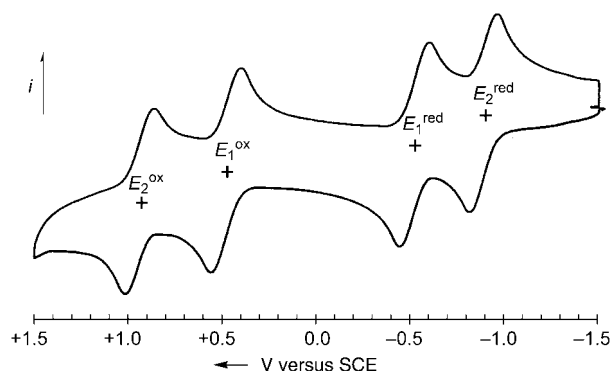
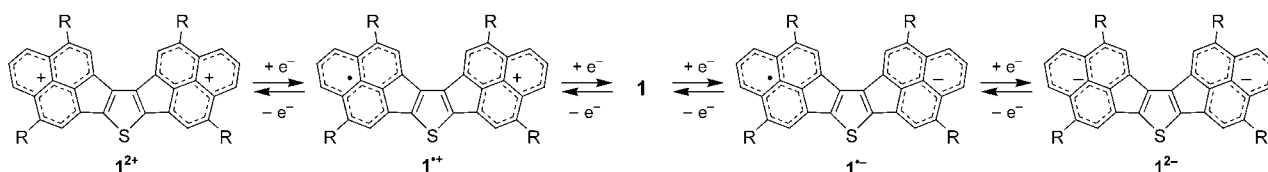
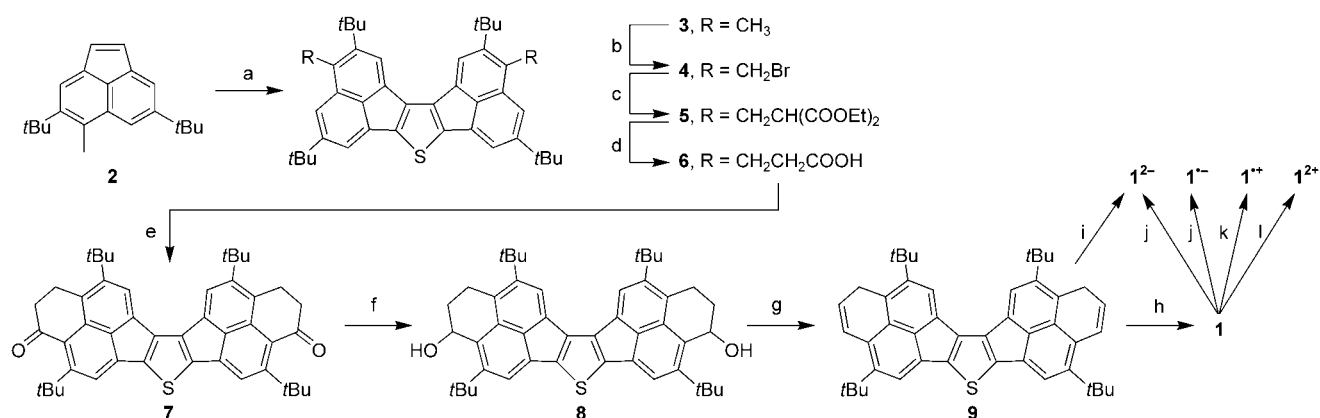


Figure 1. Cyclic voltammogram (versus saturated calomel electrode) of **1** in CH₂Cl₂ with 0.1 M Bu₄NClO₄ as the supporting electrolyte at room temperature; sweep rate = 100 mV s⁻¹.

comparable to that of pentaleno[1,2,3-*cd*;4,5,6-*c'd'*]diphenylene (PDPL, 0.99 V^[3b]), which is the smallest value reported for closed-shell hydrocarbons.^[1c] Thus, **1** possesses a high amphoteric redox ability, which indicates that it has a small HOMO–LUMO gap. Such a small gap is also confirmed by the electronic absorption spectrum of **1**, where an extraordinarily low energy band at 800–2000 nm is seen (Figure 2). The band is assignable to a HOMO–LUMO transition, which is consistent with the value of 1520 nm ($f = 0.08$) calculated by time-dependent density functional theory (TD-DFT; RB3LYP/6-31G**) calculations.^[4] The low energy band is independent of the sample concentration (5×10^{-4} and 5×10^{-5} mol L⁻¹) and the solvent polarity (cyclohexane, tetrahy-



Scheme 1. Four-stage amphoteric redox behavior of **1**.



Scheme 2. Synthesis of neutral **1** and ionic redox species **1**²⁺, **1**^{•+}, **1**^{•-}, and **1**²⁻. Reaction conditions: a) Sulfur, DMF, reflux, 2 h, 90%; b) *N*-bromosuccinimide (NBS), benzoyl peroxide, benzene, reflux, 10 min; c) NaOEt, CH₂(CO₂Et)₂, benzene+ethanol, RT, 21 h, 67% (2 steps); d) 1. 10% aq KOH, ethanol, reflux, 3 h, 2. 3 N HCl, reflux, 12 h, 89%; e) 1. (COCl)₂, reflux, 2 h, 2. AlCl₃, CH₂Cl₂, -30 °C, 2 h, 75%; f) AlH₃, THF, RT, 4 h, 86%; g) cat. *p*-toluenesulfonic acid, benzene, reflux, 5 min, 99%; h) *p*-chloranil, benzene, reflux, 5 min, 87%; i) KH, under vacuum, THF, RT, 1 week; j) K mirror, THF, RT; k) 1 equiv. of SbCl₅, CH₂Cl₂; l) D₂SO₄, RT, 10 days.

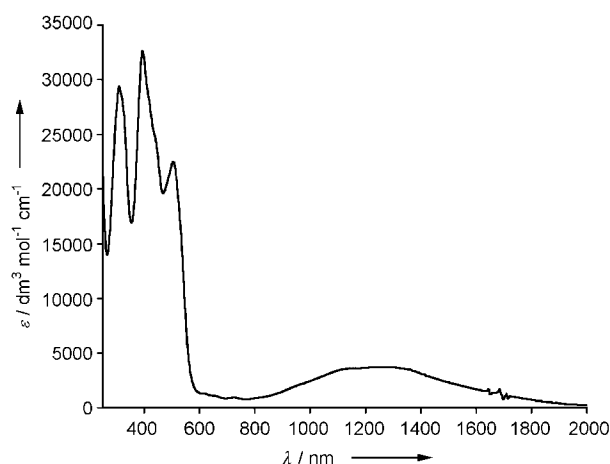


Figure 2. Electronic absorption spectrum of **1** in CH₂Cl₂ at room temperature.

dofuran, dichloromethane, and acetonitrile). Such observations exclude the possibility that the band is an intermolecular charge-transfer (CT) absorption band.

The high amphotericity indicates that **1** should yield cationic and anionic species readily. The ionic redox species of **1** were generated with no difficulties and showed no appreciable decomposition over several weeks at room temperature. The reaction conditions are summarized in Scheme 1. The monovalent radical species **1**^{•+} and **1**^{•−} gave rise to well-resolved ESR signals without detectable changes in the spectra at 183–293 K. The coupling constants of the ring protons are given in Table 1 along with the theoretical

Table 1: Experimental and theoretical hyperfine coupling constants (in mT) of **1**^{•+} and **1**^{•−}.

position	1 ^{•+} [a]		1 ^{•−} [b]	
	exptl.	theor. [c]	exptl.	theor. [c]
1,11	0.218	−0.225	0.150	−0.163
2,10	0.060	+0.045	0.004	+0.004
3,9	0.218	−0.204	0.154	−0.164
5,7	0.029	+0.003	0.068	+0.045
13,14	0.060	+0.054	0.008	−0.004

[a] Recorded in CH₂Cl₂ at −70 °C. The *g* value was 2.0045. [b] Recorded in THF at −70 °C. The *g* value was 2.0034. [c] Calculated at the SVWN/6-31G** level and with the McConnell equation (*Q* = −2.5 mT for **1**^{•+} and −2.4 mT for **1**^{•−}).

coupling constants calculated by the DFT (SVWN/6-31G**) method and the McConnell equation.^[5] The agreement between the experimental and the theoretical hyperfine coupling constants indicates that the unpaired electron is not confined to one phenalenyl moiety (A) but is delocalized over the entire molecule (B).^[6] The spin-density calculation indicates that the π spin of **1**^{•+} and **1**^{•−} resides on the two phenalenyl moieties with a similar spin distribution pattern to that of the phenalenyl radical (Figure 3). The similarity of the distribution pattern on two phenalenyl moieties supports the idea that both the HOMO and LUMO of **1** should have a

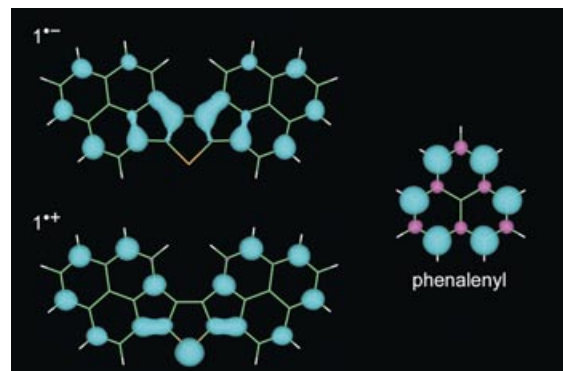
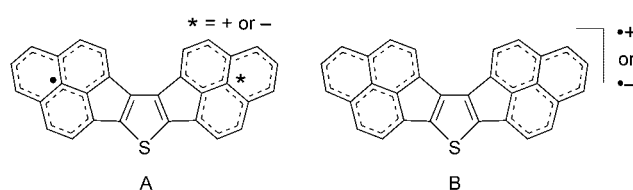


Figure 3. Spin density of **1**^{•+}, **1**^{•−}, and the phenalenyl radical calculated at the SVWN/6-31G** level.

large contribution from the nonbonding molecular orbital (NBMO) in the phenalenyl radical.

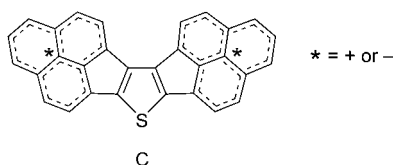
The π -charge distribution of the divalent species **1**²⁺ and **1**^{2−} should closely relate to the π -spin distribution of the monovalent species **1**^{•+} and **1**^{•−}. The removal and addition of two electrons in the divalent species occurs in the same molecular orbitals as those of a single electron in the monovalent species, that is the HOMO and LUMO, respectively. The divalent species **1**²⁺ and **1**^{2−} gave rise to only seven signals in the ¹H NMR spectra (two from the *tert*-butyl groups and five from the ring protons; Table 2). This simple ¹H NMR

Table 2: ¹H and ¹³C NMR spectroscopic data (δ) of **1**²⁺ and **1**^{2−}, and ¹³C NMR chemical shift changes on going from **1**²⁺ to **1**^{2−}. [a]

position	1 ²⁺		1 ^{2−}		position [b]	$\Delta\delta_c$ [c]
	¹ H	¹³ C	¹ H	¹³ C		
1,11	8.75	148.8	8.08	115.4	α	33.4
2,10	7.39	131.0	7.50	118.2	β	12.8
3,9	8.75	150.0	8.06	115.7	α	34.3
3a,8a		134.0		129.6		4.4
4,8		185.0		128.8	α	56.2
5,7	7.14	123.6	8.07	116.0	β	8.6
5a,6b		155.2		111.1	α	44.1
8c,15c		139.0		127.8		11.2
13a,13d		147.6		108.7	α	38.9
13,14	7.27	125.0	8.93	119.2	β	5.8
12,15		180.0		128.1	α	51.9
11a,15a		133.9		129.9		4.0
8b,15b		129.1		129.5		−0.4
5b,6a		159.5		119.7		39.8
13b,13c		150.4		123.4		27.0

[a] Compound **1**²⁺ was recorded in D₂SO₄ at room temperature. Compound **1**^{2−} was recorded in [D₈]THF at room temperature. [b] α and β denote the positions shown in the first formula. [c] $\Delta\delta_c = {}^{13}\text{C}(\text{1}^{2+}) - {}^{13}\text{C}(\text{1}^{2-})$.

spectroscopic pattern reflects the C_2 -symmetry of the divalent species. The changes in the ^{13}C NMR chemical shifts of the sp^2 carbon atoms on going from $\mathbf{1}^{2+}$ to $\mathbf{1}^{2-}$ are 744.0 ppm (or 186.0 ppm per electron), which supports the complete generation of the dication and the dianion.^[7] The changes observed in chemical shifts for the individual carbon atoms are large at the α position and small at the β position. A similar trend is found with the changes found for the chemical shifts for the phenalenyl species: large (51.8 ppm) at the α position and small (4.9 ppm) at the β position.^[8] These NMR spectroscopic studies show that the electronic structures of the phenalenyl cation and anion contribute largely to the divalent species $\mathbf{1}^{2+}$ and $\mathbf{1}^{2-}$, as shown in formula C. Thus, it can be concluded that the high amphotericity of $\mathbf{1}$ results from the NBMO character of its frontier orbitals.



A large exchange interaction ($K_{\text{H,L}}$) in the frontier orbitals is expected for a compound with a small HOMO–LUMO gap and a large spatial overlap between these orbitals which would lead to a pronounced biradical character.^[9] The frontier orbitals in the two phenalenyl moieties in $\mathbf{1}$ have a very similar pattern to the NBMO of the phenalenyl radical, and therefore substantial spatial overlap between the HOMO and LUMO is expected (Figure 4). ESR measurements of solid $\mathbf{1}$ afforded a

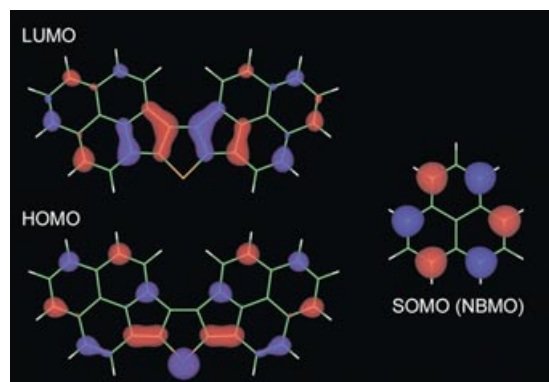


Figure 4. HOMO and LUMO of $\mathbf{1}$ as well as the singly occupied molecular orbital (SOMO) of the phenalenyl radical calculated at the B3LYP/6-31G** level.

typical spectra for triplet species ($|D| = 17.2$ mT, $|E| = 3.9$ mT). Furthermore, the temperature dependence of the half-field signal indicated a thermal excitation to the triplet state with an energy gap ($\Delta E_{\text{S-T}}$) of ~ 5 kJ mol $^{-1}$. The average distance between the two interacting spins is estimated from the D value to be 5.5 Å, which is smaller than the intramolecular distance between the centers of the two phenalenyl moieties of $\mathbf{1}$ (8.4 Å). This finding suggests that an unpaired

electron is not confined to one phenalenyl moiety but can delocalize on the central thiophene ring. The unpaired electron spin of a triplet state generally broadens NMR resonance signals by thousands of hertz. No signals arising from the ring protons were observed in the ^1H NMR spectrum of $\mathbf{1}$ recorded in CD_2Cl_2 . Although a weak and broad signal was recognized between 4 and 9 ppm below -70°C , sharp signals could not be obtained even at -90°C (see the Supporting Information). An equilibrium with the thermally accessible triplet state would cause line broadening of the NMR resonance signals. Such a thermal accessibility to the triplet state supports the existence of a small HOMO–LUMO gap and the large exchange interaction ($K_{\text{H,L}}$) in $\mathbf{1}$.

The large exchange interaction ($K_{\text{H,L}}$) is another fascinating property that describes the ground-state configuration.^[10] A configuration interaction (CI) calculation at the CASSCF(2,2)/6-31G(d,p) level afforded an admixture (4%) of the double excitation $^1\Phi_{\text{H,H} \rightarrow \text{L,L}}$ into the ground configuration $^1\Phi_0$. The singlet diradical index, proposed by Neese and co-workers recently,^[11] was estimated to be approximately 35% based on the CI calculation for $\mathbf{1}$. The singlet diradical picture was supported by the DFT calculation at the UB3LYP/6-31G(d,p) level, which afforded an energy lowering of 7 kJ mol $^{-1}$ induced by symmetry breaking of the DFT solution. Fortunately, we obtained two indicative results for the singlet biradicaloid character.

The first indicative result is the X-ray crystal structure showing that $\mathbf{1}$ formed two kinds of dimeric pairs with substantially short nonbonding contacts of about 3.1 Å between each thiophene ring, as shown in Figure 5. The terminal rings were separated by over 4.2 Å because of the steric repulsion between the *tert*-butyl groups and the six-membered rings. The van der Waals contact between carbon atoms only exist within the central dicyclopenta[*b*; *d*]thiophene moieties. The attractive forces leading to dimerization would probably be an intermolecular CT interaction. Therefore, there will be intermolecular delocalization of electrons in the dimer of $\mathbf{1}$.^[12] There are two possible explanations for

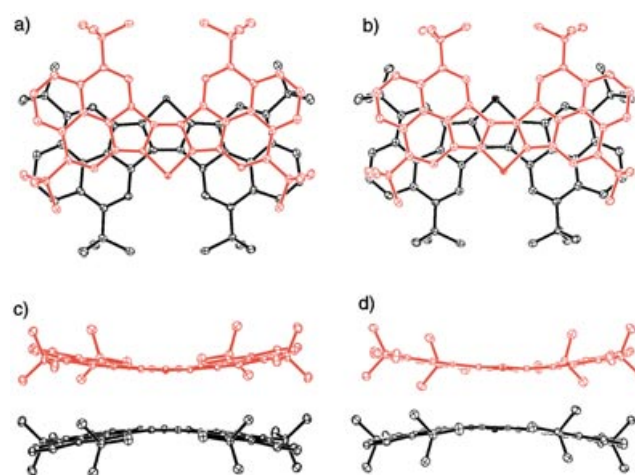


Figure 5. Crystal structures of $\mathbf{1}$. Top view of the dimeric pair A (a) and B (b), and side view of the dimeric pair A (c) and B (d). Hydrogen atoms are omitted for clarity.

the dimerization of **1** through CT interactions: The first is the attractive forces resulting from electron transfer between occupied and unoccupied molecular orbitals (MOs) in each of the monomers in the dimers. In general, the most important terms are related to an intermolecular HOMO–LUMO interaction; however, with **1** the HOMO–LUMO interaction should lead to no or only slight stabilization of the system because of the orbital symmetry mismatching in the dimeric arrangement described above. In contrast, the next highest occupied molecular orbital (NHOMO)–LUMO interaction should result in the formation of a bonding intermolecular orbital (Figure 6a). The second explanation is an attractive

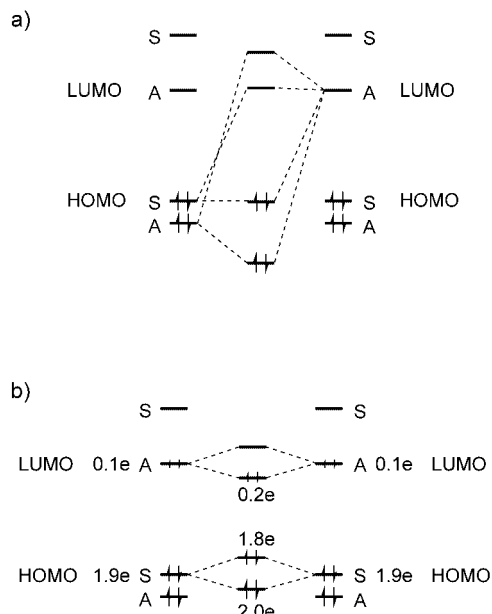
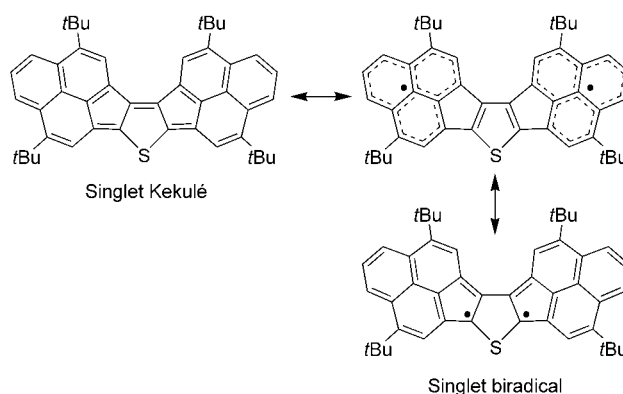


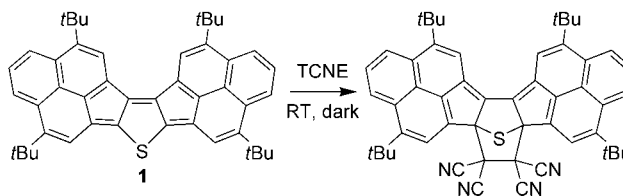
Figure 6. Schematic drawing of the molecular orbital interaction of dimeric **1** through electron transfer between occupied and unoccupied molecular orbitals (a), and through the double excitation configuration $^1\Phi_{H,H\rightarrow L,L}$ (b). S and A denote the symmetry of the molecular orbitals.

interaction through the double excitation configuration $^1\Phi_{H,H\rightarrow L,L}$, that is, a singlet biradical contribution. Based on the CASSCF(2,2) calculation of **1**, the occupation numbers of HOMO and LUMO are 1.9 and 0.1, respectively. In this case, a LUMO–LUMO interaction will lead to stabilization of the system because a newly formed “LUMO” of the dimer, which is more stable than the original LUMO, can accommodate at least 0.2 electrons (Figure 6b). In addition, a HOMO–HOMO interaction seems likely to stabilize the system because a newly formed “HOMO” of the dimer would contain only 1.8 electrons. This would suppress a four-electron repulsion that would result from the interaction between fully occupied orbitals. A valence-bond picture is helpful for understanding the singlet biradical structure. The Kekulé form of **1** loses aromatic stabilization in the central thiophene ring, whereas thiophene and phenalenyl radical structures appear in a singlet biradical form of **1**. Therefore, mixing of the singlet biradical configuration with the ground state is promoted. The broken symmetry DFT solution affords a large π -spin population on the phenalenyl moieties



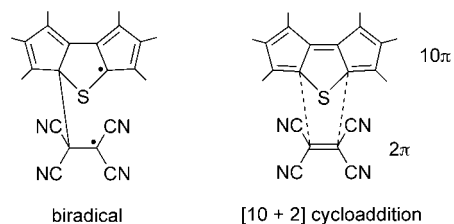
with a little delocalization to the thiophene ring (see the Supporting Information).

The second indicative result is a cycloaddition reaction of **1** with tetracyanoethylene (TCNE). Mixing a solution of **1** and TCNE in C_6D_6 exclusively afforded a TCNE adduct within 10 seconds in the dark at room temperature (Scheme 3). The



Scheme 3. Reaction of **1** with tetracyanoethylene (TCNE).

structure of the adduct was confirmed by NMR spectroscopy (1H , ^{13}C , NOESY, HMBC, and HMQC experiments). The reaction may proceed by a stepwise process involving a biradical or a symmetry-forbidden thermal concerted [10+2] process. At this stage the reaction mechanism is still



undetermined. However, discussion of symmetry being “forbidden” or “allowed” becomes meaningless for the concerted reaction of biradicaloid compounds because the double excitation configuration should lower the symmetry-imposed activation energy.^[9]

In conclusion, the amphoteric redox compound **1** was prepared by a stepwise synthesis and showed highly amphoteric redox properties. Notably, a singlet biradical character of **1** is suggested by quantum chemical calculations and supported by experimental results. The chemistry of amphoteric redox systems are expected to contribute to investigations

into the solid-state properties of conjugated singlet biradicals, such as crystal packing, magnetism, and electroconductive behavior. Closed-shell conjugated systems based on the phenalenyl radical could lead to conjugated biradicaloid compounds that could be isolated in the air.

Experimental Section

The detailed synthetic procedure for **1** is described in the Supporting Information.

Crystal data for **1**: $C_{52}H_{60}S$, $M = 717.11$, triclinic, space group $P\bar{1}$ (no. 2), $a = 12.901(2)$, $b = 17.000(3)$, $c = 20.674(4)$ Å, $\alpha = 82.243(3)$, $\beta = 89.589(3)$, $\gamma = 69.229(3)^\circ$, $V = 4196(1)$ Å³, $Z = 4$, $\mu(Mo_{K\alpha}) = 0.111$ cm⁻¹, $\rho_{\text{calcd.}} = 1.135$ g cm⁻³, $R1(wR2) = 0.071$ (0.187) for 982 parameters and 15174 unique reflections with $I > 2\sigma(I)$, GOF = 1.004. Data collection were performed on Enraf-Nonius CAD-4 diffractometer ($Mo_{K\alpha}$, $\lambda = 0.71069$ Å) at 9 K. The structure was solved with direct methods and refined with full-matrix least squares (teXsan). CCDC-237621 contains the supplementary crystallographic data for this paper. These data can be obtained free of charge from www.ccdc.cam.ac.uk/conts/retrieving.html (or from the Cambridge Crystallographic Data Centre, 12 Union Road, Cambridge CB21EZ, UK; fax: (+44) 1223-336-033; or deposit@ccdc.cam.ac.uk).

Received: May 6, 2004

Keywords: charge transfer · conjugation · density functional calculations · radicals · redox chemistry

P. M. W. Gill, B. G. Johnson, W. Chen, M. W. Wong, J. L. Andres, M. Head-Gordon, E. S. Replogle, J. A. Pople, Gaussian, Inc., Pittsburgh, PA, 1998.

- [5] H. M. McConnell, *J. Chem. Phys.* **1956**, 24, 764.
- [6] The highly delocalized structure of the charge and the spin suggests that the monovalent radicals $1^{\bullet+}$ and $1^{\bullet-}$ can be placed in the class III category in the classification of mixed-valence species, which is consistent with the quite large values between the first and the second redox potentials ($E_2^{\text{ox}} - E_1^{\text{ox}} = 0.47$ V, $E_1^{\text{red}} - E_2^{\text{red}} = 0.37$ V). The properties of mixed valence compounds depend on the extent of the electronic interaction between the redox centers and its range. The common classification is: small or nonexistent (class I), slight (class II), and strong interaction (class III, including the completely delocalized molecules). See M. B. Robin, P. Day, *Adv. Inorg. Chem. Radiochem.* **1967**, 10, 247.
- [7] H. Spiesecke, W. G. Schneider, *Tetrahedron Lett.* **1961**, 2, 468.
- [8] I. Sethso, D. Johnels, U. Edlund, A. Sygula, *J. Chem. Soc. Perkin Trans. 2* **1990**, 1339.
- [9] The term “ π , π -biradicaloid” was used previously for a compound possessing two approximately nonbonding π -orbitals. See, J. Kolc, J. Michl, *J. Am. Chem. Soc.* **1973**, 95, 7391.
- [10] D. R. McMasters, J. Wirz, *J. Am. Chem. Soc.* **2001**, 123, 238.
- [11] D. Herebian, K. E. Wieghardt, F. Neese, *J. Am. Chem. Soc.* **2003**, 125, 10997.
- [12] In general, the π - π interactions of aromatic systems is affected by various electronic factors. The well-known attractive forces are derived from electrostatic interactions between electron-deficient and electron-rich sites. However, this interaction is not likely to be effective in the dimeration of **1** because there is only a small overlap of positive and negative charges as found from the Mulliken charge analysis (see the Supporting Information).

- [1] a) K. Nakasuji, K. Yoshida, I. Murata, *J. Am. Chem. Soc.* **1982**, 104, 1432; b) K. Nakasuji, K. Yoshida, I. Murata, *Chem. Lett.* **1982**, 969; c) K. Nakasuji, K. Yoshida, I. Murata, *J. Am. Chem. Soc.* **1983**, 105, 5136; d) I. Murata, S. Sasaki, K.-U. Klabunde, J. Toyoda, K. Nakasuji, *Angew. Chem.* **1991**, 103, 198; *Angew. Chem. Int. Ed. Engl.* **1991**, 30, 172; e) K. Ohashi, T. Kubo, T. Masui, K. Yamamoto, K. Nakasuji, T. Takui, Y. Kai, I. Murata, *J. Am. Chem. Soc.* **1998**, 120, 2018; f) T. Kubo, K. Yamamoto, K. Nakasuji, T. Takui, *Tetrahedron Lett.* **2001**, 42, 7997; g) T. Kubo, K. Yamamoto, K. Nakasuji, T. Takui, I. Murata, *Angew. Chem.* **1996**, 108, 456; *Angew. Chem. Int. Ed. Engl.* **1996**, 35, 439; h) T. Kubo, K. Yamamoto, K. Nakasuji, T. Takui, I. Murata, *Bull. Chem. Soc. Jpn.* **2001**, 74, 1999.
- [2] J. Nakayama, Y. Ito, *Sulfur Lett.* **1989**, 9, 135.
- [3] a) To evaluate the amphoteric redox abilities of a molecule, the numerical sum (E^{sum}) of the oxidation potential (E^{ox}) and the reduction potential (E^{red}), $E^{\text{sum}} = E^{\text{ox}} + (-E^{\text{red}})$, is used; see V. D. Parker, *J. Am. Chem. Soc.* **1976**, 98, 98, and ref [1a]. b) The measurement condition for PDPL is different from that for **1**. The condition for PDPL is as follows; temperature, -50°C ; solvent, DMF; supporting electrolyte, 0.1M Et_4NClO_4 , sweep rate, 30 mVs⁻¹; working electrode, Pt; reference electrode, saturated calomel electrode (SCE).
- [4] All DFT and CASSCF calculations were done using Gaussian 98 (Revision A.7), M. J. Frisch, G. W. Trucks, H. B. Schlegel, G. E. Scuseria, M. A. Robb, J. R. Cheeseman, V. G. Zakrzewski, J. A. Montgomery, R. E. Stratmann, J. C. Burant, S. Dapprich, J. M. Millam, A. D. Daniels, K. N. Kudin, M. C. Strain, O. Farkas, J. Tomasi, V. Barone, M. Cossi, R. Cammi, B. Mennucci, C. Pomelli, C. Adamo, S. Clifford, J. Ochterski, G. A. Petersson, P. Y. Ayala, Q. Cui, K. Morokuma, D. K. Malick, A. D. Rabuck, K. Raghavachari, J. B. Foresman, J. Cioslowski, J. V. Ortiz, B. B. Stefanov, G. Liu, A. Liashenko, P. Piskorz, I. Komaromi, R. Gomperts, R. L. Martin, D. J. Fox, T. Keith, M. A. Al-Laham, C. Y. Peng, A. Nanayakkara, C. Gonzalez, M. Challacombe,